PCCP

Accepted Manuscript

ROYAL SOCIETY OF CHEMISTRY

www.rsc.org/pccp

Fluorescence response of a dipolar organic solute in a dicationic ionic liquid (IL): Is the behavior of dicationic IL different from that of usual monocationic IL?

Prabhat Kumar Sahu, Sudhir Kumar Das and Moloy Sarkar*

School of Chemical Sciences

National Institute of Science Education and Research

Bhubaneswar 751005, India

* Corresponding author, School of Chemical Sciences, National Institute of Science Education and Research, Bhubaneswar 751005, India. Fax: +91-674-2304050. Tel: +91-674-2304037. Email:msarkar@niser.ac.in

Abstract

Solvation and rotational relaxation dynamics of coumarin 153 has been investigated in a dicationic ionic liquid, 1,6-bis-(3-methylimidazolium-1-yl)hexane bis-(trifluoromethylsulfonyl)amide ($[C_6(MIm)_2][NTf_2]_2$), for the first time to have a comprehensive and a quantitative understanding of the nature of ionic fluid and its influence on the average solvation and rotational relaxation time. In several occasions photophysical data obtained in the present dicationic IL have also been compared with the monocationic imidazolium-based ionic liquid so as to find out the difference in their behavior. The dicationic ionic liquid has been synthesized via a two step process and subsequently characterized by conventional spectroscopic methods. Steady state absorption and fluorescence measurements reveal that the polarity of the ionic liquid is close to that of dichloromethane. A steady state excitation wavelength dependent fluorescence measurement indicates micro-heterogeneous nature of the ionic liquid. However, the steady state excitation wavelength dependent fluorescence response is found to be similar for both dicationic and a structurally similar monocationic ionic liquid. In the time-resolved fluorescence studies, contrary to monocationic imidazolium-based ionic liquid, no missing ultra-fast component of solvation has been observed in the present dicationic IL. Excitation wavelength dependence of the average solvation and rotation times also indicates the micro-heterogeneous nature of theses media. When viscosity dependence (η) of the measured average solvation $<\tau_s>$ and rotation $<\tau_r>$ times are verified by the relation: $<\tau_x> \propto (\eta/T)^p$ (x being solvation or rotation, p is the exponent and T is the temperature), the fractional dependence of both average solvation and rotational times with the medium viscosity have been observed. The recent findings (J. Chem. Phys. 2012, 136, 174503, Chemical Physics Letters 2011,517, 180, ChemPhysChem 2012,13,2761) and the outcome of the present study suggest that the observed viscosity-diffusion (η-D) decoupling for the present dicationic ionic liquid is due to dynamic heterogeneity of the medium.

1 Introduction

In recent years, the room temperature ionic liquids (RTILs) have emerged as the specialty media that can be used in wide range of applications in diverse areas of chemical, biological and material sciences.[1-5] Quite interestingly, their applications span from organic synthesis to rocket science.[1-5] The growing usefulness of RTILs in technological applications have encouraged researchers to undertake studies that would help understand fundamental aspects of their actions. In this regard, studies on solvation dynamics have appeared to be quite popular by virtue of the fact that solute reactivity is intricately related to solvation process.[6] Studies on RTILs have revealed that solvation dynamics in ionic liquids is quite complex.[7,8] Solvation dynamics is slow in ILs as compared to conventional solvents. Solvation dynamics in ILs is also temporally dispersive [9-12] and quite similar in nature to that has been observed in supercooled liquids.[13-15] Studies have also revealed that significant portion of the spectral relaxation dynamics is quite fast (<25 ps). However, studies on solvation and rotational dynamics though found to be useful in providing a great deal of information about the microenvironment of the solute in a medium, are limited to mainly monocation-based systems.[6-50] The dicationic ionic liquids with their unique properties such as higher thermal stability, shear viscosity, surface tensions, and larger liquid density are expected to be advantageous over the traditional monocationic ILs as far as technological applications are concerned. A comprehensive study of solvation and rotational relaxation dynamics in dicationic based system is expected to provide new insights into the fundamentals of solvation and rotational relaxation phenomena which in turn may help in exploring exotic applications of these dicationic based IL systems.

Very recently dicationic ionic liquids have attracted considerable attention and consequently ILs comprising imidazolium,[51-55] ammonium and pyridinium-based [56-61] dicationic ILs have been

developed. Armstrong [51] and Shirota[55] have extensively studied physical properties of several dicationic based ionic liquids. These studies when compared with their monocationic counterpart reveal that density, viscosity, surface tension, glass transition temperature, melting point and thermal stability of the dicationic systems are appreciably higher than those of the monocationic analogues. Computer simulation studies on the dicationic ILs have also been performed.[62-66] Interestingly, Shirota and Ishida [67] while investigating interionic vibrations using femtosecond optical-heterodyne-detected Raman-induced Kerr effect spectroscopy (OHD-RIKES) have observed difference in the low-frequency Kerr spectral profiles between the monocationic 1-methyl-3-propylimidazolium bis-(trifluoromethylsulfonyl)amide ($[C_3MIm][NTf_2]$) and the dicationic IL, 1,6-bis-(3-methylimidazolium-1-yl)hexane bis-(trifluoromethylsulfonyl)amide ($[C_6(MIm)_2][NTf_2]_2$). They attributed this inhomogeinity due to the segregation in microstructures of dicationic ILs with longer alkyl-linker-chain length. The study further suggested that dynamical heterogeneous behavior of dicationic IL correlates strongly with structural variation. While carrying out molecular dynamics (MD) simulation studies on a series of germinal dicationic ILs, Bodo et al.[65] have observed many common characteristics with corresponding monoimidazolic ILs. In a recent study Li et al.[66] have shown that for short alkyl chain, the cations in dicationic ionic liquids and monocationic ionic liquids exhibit very similar structural nano-organization and heterogeneity whereas significant difference in structural heterogeneity is observed for medium and long-chain dicationic and monocationic ionic liquids. Above reports demonstrate that majority of the work carried out on dicationic ionic liquids are through computer simulations and are mainly aimed at finding structural nano-organization and micro-heterogeneous behavior of this medium. Experimental studies aiming at the same objective have not been carried out. Moreover, it is also evident from the above reports that

studies on solvation and rotational relaxation in RTIL comprising the dicationic moiety are elusive. Since the dynamical behavior of the dicationic ionic liquid is perceived to be considerably different from their monocationic counterpart, it would be interesting to study solvation and rotational relaxation dynamics in this media. These studies are expected to provide more information about molecular charge transfer processes and frictional effect on solute motions.[68]

In view of the above facts, we have investigated solvation and rotational relaxation dynamics of coumarin153 (C153) in a dicationic RTIL, 1,6-bis-(3-methylimidazolium-1-yl)hexane bis-(trifluoromethylsulfonyl)amide ($[C_6(MIm)_2][NTf_2]_2$) through steady state and time-resolved fluorescence spectroscopy. The ionic liquid was synthesized and rigorously purified by us for optical studies. The structures of the IL and the probe are shown in Scheme 1.

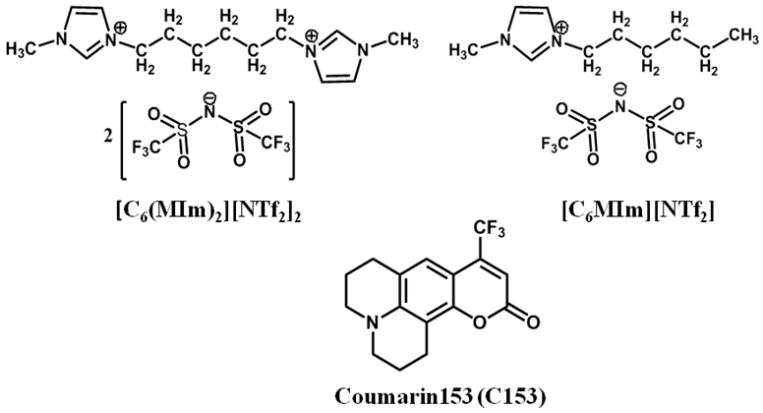

Scheme 1. Structures of the RTIL and Coumarin 153 (C153)

2 Experimental Section

Materials: Coumarin 153 (C153) (laser grade, Exciton) was used as received. The dicationic RTIL $[C_6(MIm)_2][NTf_2]_2$ was synthesized by following the procedure of Shirota.[55] Purity of the RTIL was checked by ^{1}H NMR spectroscopy (see ESI† Fig. S1) and viscosity data were matched

with literature data.[55] The dicationic RTIL was kept in high vacuum for two days before use. The RTILs were transferred into different long-necked quartz cuvette and requisite amount of C153 was added to prepare the solution taking precaution to avoid moisture absorption by this media. The long-necked quartz cuvette was sealed with septum and parafilm to further ensure dry condition.

Synthesis of dicationic ionic liquid $[C_6(MIm)_2][NTf_2]_2$

1. 1,6-Bis(3-methylimidazolium-1-yl)hexane bromide, $[C_6(MIM)_2][Br]_2$ (precursor for target IL): 1, 6-Dibromohexane (25 gm, 102.5 mmol) was gradually added to an acetonitrile solution (50 mL) of 1-methylimidazole (22 gm, 267.9 mmol) in a round-bottom flask equipped with a reflux condenser. The solution was stirred under nitrogen atmosphere at 343 K for 3 days. The solution was then condensed by evaporation, and was washed by diethyl ether. A brown colored salt was precipitated. The salt was then recrystallized from diethyl ether for several times. After drying under vacuum at 308 K, the final product was obtained as a white solid. The yield was 88%.^{1}H-NMR (DMSO-d_6, 400 MHz, TMS): δ (ppm) = 9.28 (s, 2H), 7.83 (s, 2H), 7.74 (s, 2H), 4.20(t, 4H), 3.86(s, 6H), 1.80(m, 4H), 1.28(m, 4H).

2.1,6-Bis(3-methylimidazolium-1-yl)hexanebis(trifluoromethylsulfonyl)amide, $[C_6(MIM)_2][NTf_2]_2$: Aqueous solution of lithium bis(trifluoromethylsulfonyl)amide solution (8.5 gm, 29.6 mmol in 30 mL water) was gradually added to the aqueous solution of $[C_6(MIM)_2][Br]_2$ (5.74 gm, 14.1 mmol in 50ml water). The mixture was stirred at room temperature for 1 day and subsequently the aqueous solution was decanted. The organic layer was dissolved in ethyl acetate (30 mL) and was washed with water (30 mL × 5). The organic layer was dried with anhydrous Na_2SO_4. Then the solvent was evaporated and the residue was

mixed with activated charcoal in acetonitrile. The activated charcoal was removed by filtration, and the remaining solvent was also evaporated. The charcoal treatment was repeated twice. Finally a colourless viscous liquid was obtained. The viscous liquid was then dried under vacuum at 308 K for 3 days. The yield was 88%. ^{1}H NMR (DMSO, 400MHz, TMS): δ(ppm)= 9.07(s, 2H), 7.73(s, 2H), 7.69(s, 2H), 4.15(t, 4H), 3.84(s, 6H), 1.79(m, 4H), 1.26(m, 4H). The ^{1}HNMR spectrum of the final compound, $[C_6(MIM)_2][NTf_2]_2$, is shown in Fig. S1(ESI†). The NMR spectrum (Fig. S1, ESI†) reveals that, aliphatic protons of alkyl linker chain appear in the range 1.26-4.15 ppm. The aromatic protons (4 and 5-position) of the two imidazolium rings appear in the range 7.69-7.73 ppm. Interestingly, C(2) H of imidazolium protons appear in more down filed region (9.07 ppm), indicating the acidic nature of the proton. Methyl protons (3-position of imidazolim ring) appear at 3.84 ppm. ESI-MS (+ve): 528.12 m/z $[C_6(MIm)_2\ NTf_2]^{+}$.

Instrumentation: The absorption and fluorescence spectra were measured using Perkin Elmer (Lambda-750) spectrophotometer and Perkin Elmer, LS 55 spectrofluorimeter respectively. The fluorescence spectra were corrected for the spectral sensitivity of the instrument. For steady-state experiments, all samples were excited at different excitation wavelength from 350 to 490nm including 375, 405 and 445nm. Time-resolved fluorescence measurements were carried out using a time-correlated single-photon counting (TCSPC) spectrometer (Edinburgh, OB920). The samples were excited at 375 nm, 405nm and 445 nm using different picoseconds laser diode (EPL), and the signals were collected at magic angle (54.7°) using a Hamamatsu microchannel plate photomultiplier tube (R3809U-50). The lamp profile was recorded by scatterer (dilute ludox solution in water) in place of the sample. The instrument response functions (FWHM) of our setup were ~75 ps for 375 nm, 95 ps for 405 nm and 445 nm picoseconds diode laser respectively. Decay curves were analyzed by nonlinear least-squares iteration procedure using

F900 decay analysis software. The qualities of the fit were judged by the chi square (χ^2) values and weighted deviations were obtained by fitting. The same setup was used for anisotropy measurements. The emission intensities at parallel (I_{II}) and perpendicular ($I_{\perp}$) polarizations were collected alternatively until peak difference between parallel (I_{II}) and perpendicular ($I_{\perp}$) decay (at t = 0) ~5000 was reached. For G-factor calculation, the same procedure was adopted, but with 5 cycles and horizontal polarization of the exciting laser beam. The same software was also used to analyze the anisotropy data. The temperature was maintained by circulating water through the cell holder using a Quantum, North West (TC 125) temperature controller. The viscosities of the RTIL were measured by LVDV-III Ultra Brookfield Cone and Plate viscometer (1% accuracy and 0.2% repeatability).

Method: The time-resolved decay profiles were measured at 5/10 nm intervals across the entire steady-state emission spectra at magic angle (54.7°). The total numbers of measurements were 27-30 in each case. For deconvoluting the instrument response function, each decay curve was fitted by using a triexponential decay function to obtain deconvolutes the instrument response function and to obtain a χ^2 value between 1 and 1.2 which indicated the goodness of fit. The collected intensity decays at magic angle had been analyzed using a standard method.[69] The emission maximum at each time $\bar{\nu}(t)$ was obtained by fitting the spectrum to a log-normal line-shape function which is given below

$$I = h\, exp[-ln2\{ln(1+\alpha)/\gamma\}^2] \quad (1)$$

for $\alpha > -1 = 0$ and $I = 0$ for $\alpha \leq -1$

where $\alpha = 2\gamma\,(\bar{\nu} - \bar{\nu}_{peak})/\Delta$, $\bar{\nu}_{peak}$ is the wavenumber corresponding to the peak, h is the peak height, Δ is the full width at half maximum (FWHM) and γ is a measure of the asymmetry of the band shape. Optimizing these four parameters by nonlinear least squares iteration, the best fitted curve was obtained.

The peak frequencies obtained from the log-normal fitting of time resolved emission spectra (TRES) were then used to construct the decay of solvent correlation function (*C (t)*) which is given below.

$$C(t) = \frac{\bar{\nu}(t) - \bar{\nu}(\infty)}{\bar{\nu}(0) - \bar{\nu}(\infty)} \qquad (2)$$

where $\bar{\nu}(\infty)$, $\bar{\nu}(0)$ and $\bar{\nu}(t)$ are the peak frequencies at times infinity (∞), zero (t =0) and t respectively. The plot of *C(t)* against t (time) was fitted by a biexponential function as given below,

$$C(t) = a_1 e^{-t/\tau_1} + a_2 e^{-t/\tau_2} \qquad (3)$$

where τ_1 and τ_2 are the solvent relaxation time and a_1 and a_2 are normalized preexponential factors. The average solvation time were calculated by using the relation

$$\langle \tau_{av} \rangle = a_1\tau_1 + a_2\tau_2 \qquad (4)$$

We had also fitted *C(t)* by the stretched exponential function shown below.

$$C(t) = exp(-(t/\tau_{solv})^{\beta}) \qquad (5)$$

where $0<\beta\leq 1$

$$\langle \tau_{st} \rangle = \frac{\tau_{solv}}{\beta}\Gamma(\beta^{-1}) \qquad (6)$$

where Γ was gamma function and τ_{st} was the average solvation time considering *C(t)* was a stretched exponential function.

Time-resolved fluorescence anisotropy (r(t)) is estimated by the following equation

$$r(t) = \frac{G\ I_{VV}(t) - I_{VH}(t)}{GI_{VV}(t) + 2I_{VH}(t)} \quad \text{where} \quad G = \frac{\sum I_{HH}(t)}{\sum I_{HV}(t)} \tag{7}$$

In the above relation G is the instrument correction factor for detector sensitivity to the polarization direction of the emission. G factor for our TCSPC set up is ~0.8 at the wavelength of detection. $I_{HH}(t)$ and $I_{HV}(t)$ are the intensity of fluorescence decays when the excitation and the emission polarizer are polarized at horizontal-horizontal and horizontal-vertical alignment respectively. $I_{VV}(t)$ and $I_{VH}(t)$ are the intensity of fluorescence decays when excitation and emission polarizer are polarized at vertical-vertical and vertical-horizontal alignment. To have better understanding on the role of viscosity on rotational diffusion of solute, we have also analyzed the results in light of Stokes-Einstein-Debye (SED) hydrodynamic theory.[70]

According to SED theory, the reorientation time (τ_r) of a non-interacting solute in a solvent continuum of viscosity η is given by

$$\tau_r^{SED} = \frac{\eta V f C}{k\ T} \tag{8}$$

In the above relation, *k* is the Boltzmann constant and *T* is absolute temperature. *V* is the van der Waals volume of the solute molecule and *C* is the boundary condition parameter, which expresses the measure of coupling between the solute and the solvent. *f* is the shape factor which accounts the nonspherical shapes of the solute molecules. The two extreme boundary conditions

are stick and slip according to SED hydrodynamic theory.[70] According to stick boundary condition *C* is unity and is applicable to solute molecules larger in size than solvent molecules. When size of the solute molecule is smaller or comparable to solvent molecule then *C* becomes less than unity. This represents slip boundary condition. In SED theory shapes of the solute molecules are usually by considered as either symmetric or asymmetric ellipsoids. For nonspherical molecules, *f* is greater than unity and the magnitude of the deviation from unity in the value of *f* describes the degree of nonspherical nature of the rotating solute. For C_{slip} calculation, we have used the probe properties that are available in literature.[22] Details of the calculation have been described in our earlier publications.[71] The van der Waals volume, shape factor, and calculated slip boundary condition parameter for C153 are 243Å^3, 1.5 and 0.18 respectively.[22,71]

3 Results and Discussion

3.1. Steady state behavior of C153 in RTILs

Absorption spectrum of neat $[C_6(MIm)_2][NTf_2]_2$ is shown in Fig. 1.The absorption and emission spectra of C153 in $[C_6(MIm)_2][NTf_2]_2$ are shown in Fig. 2 along with the emission spectrum of neat ionic liquid. Comparing the emission maximum of C153 in IL and conventional media,[72] we infer that the polarity of the dicationic ionic liquid used in this study is close to that of dichloromethane. The Stokes shift as obtained from steady state spectrum of C153 are estimated to be 5060cm^{-1} in dichloromethane (DCM), 4427 cm^{-1} in dicationic IL and 4482 cm^{-1} in monocationic IL. The dynamic Stokes shift (*vide* infra) in moncationic IL (1320 cm^{-1}) is found to be very close to the value observed in DCM (1220 cm^{-1}) by Maroncelli and co-workers. Hence, from the Stokes shift values we can infer that the polarities of the ILs are close to that of

DCM. However, we stress that the studies on dielectric relaxation measurements on these ILs would be helpful to get better idea about their polarity.

The absorption and emission maxima of C153 are found to not be affected by varying the temperature from 293K to 333K.

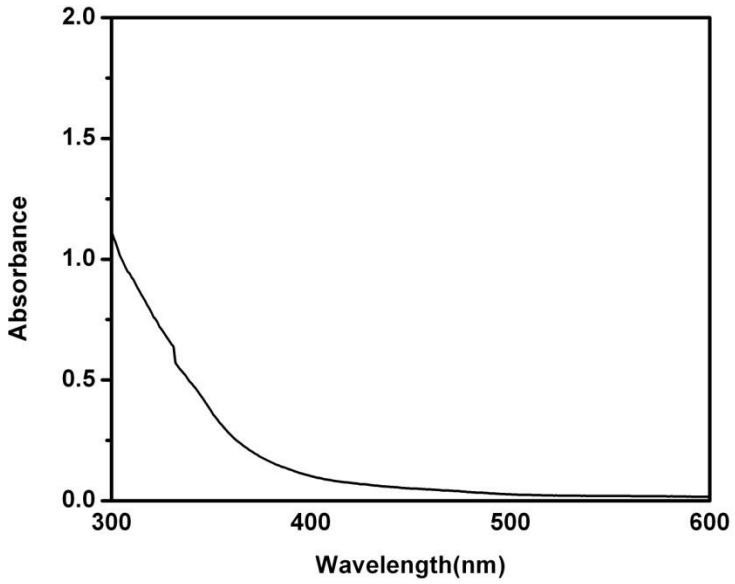

Fig. 1. Absorption spectrum of neat $[C_6(MIm)_2][NTf_2]_2$.

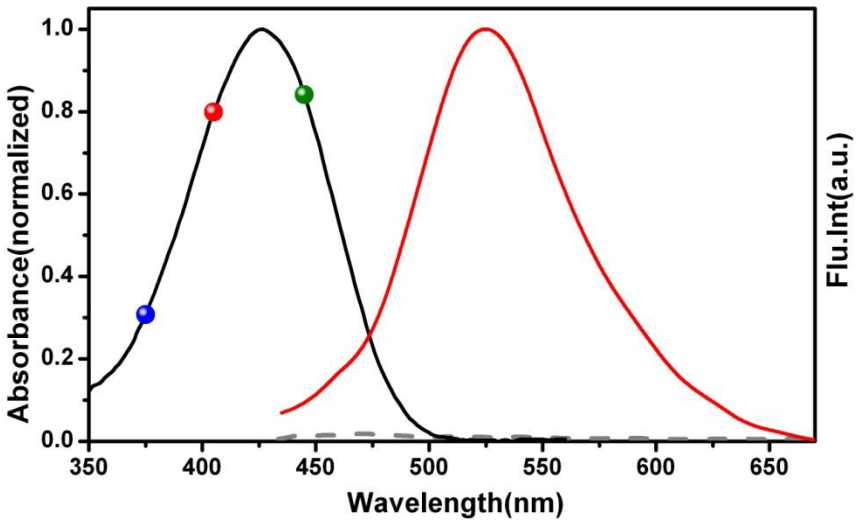

Fig. 2. Combined absorption and emission spectrum of C153 in $[C_6(MIm)_2][NTf_2]_2]$. The spectra are normalized with respect to the corresponding peak position. Blue, red and green balls denote

the excitation wavelenghths (λ_{exc}). Emission spectrum shown is for λ_{exc}=405 nm and at 293K with neat RTIL emission as dashed gray lines.

3.2. Excitation wavelength dependent fluorescence studies

The micro-heterogeneous nature of RTILs [7-8,13,16, 28-30] is investigated by following the excitation wavelength ($\lambda_{exc.}$) dependent steady state fluorescence behavior of C153 and 2-amino-7-nitrofluorene (ANF) in the IL. The choice of ANF as a probe for this study is based on the fact that relatively ANF has shorter excited state lifetime (τ) ~100 ps [7] than that of C153 (τ=3-5 ns) [72] and hence fluorescence signature of ANF in the RTIL is expected to be more responsive to those short-lived "transient" domains over which medium particles are correlated. It may be mentioned in this context that existence of different nonpolar and polar domain in ILs is believed to be the main reason behind the micro-heterogeneous nature of the medium.[7] The maximum shift of the fluorescence maxima is found to be ~8 nm for ANF and ~5 nm for C153 in $[C_6(MIm)_2][NTf_2]_2$.

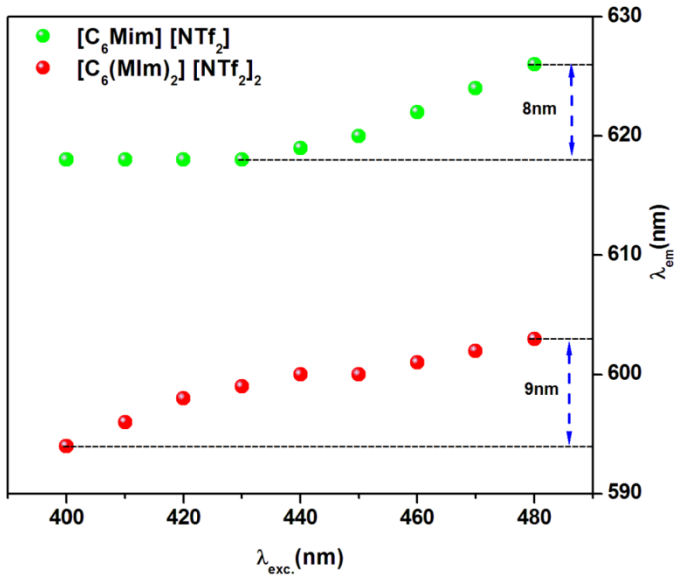

Fig. 3. Excitation wavelength dependent fluorescence response of ANF in $[C_6(MIm)_2][NTf_2]_2$ and $[C_6MIm][NTf_2]$ at 298K

Interestingly, when we compare the excitation wavelength ($\lambda_{exc.}$) dependent fluorescence behavior of ANF in the present dicationic IL $[C_6(MIm)_2][NTf_2]_2$, with a structurally similar IL, $[C_6MIm][NTf_2]$, maximum shift of the fluorescence maxima is also found to be similar (Fig. 3). We note that, this observation of red shift of the fluorescence maximum of the dipolar solutes when excited at the long-wavelength region of the absorption band, is known as "red-edge effect" (REE).[73,74] The REE events in ILs have been rationalized by considering the distribution of energetically different solvated species in the ground state and a slower rate of their solvent dependent excited-state relaxation processes.[16] Hence, the present observation also provides indirect evidence about the micro-heterogeneous nature of the dicationic ionic liquid.The changes in FWHM (full-width at half maximum) of excitation wavelength dependent emission spectra for ANF in both di and monocationic IL are also found to be similar. For a range of excitation wavelength 400 nm to 480 nm FWHM of the steady state emission spectra of ANF is estimated to be $180cm^{-1}$ and $140cm^{-1}$ in di and monocationic IL respectively. The slight difference in FWHM values in these two ILs perhaps arises due to the asymmetric broadening of the spectral envelope. In this context, we would like to mention that Ishida and Shiorta [63] while working on molecular dynamics simulation studies on dicationic and monocationic ionic liquids having different alkyl chain lengths have pointed out that the length of the nonpolar alkyl side chain has strong influence on the heterogeneous behavior. It is pertinent to mention in this context that the recent work by Cummings and co-workers [66] have also demonstrated that for short-range alkyl chain, the cations in dicationic ILs and monocationic ILs exhibit very similar structural nano-organization and heterogeneity. These recent findings and the outcome of the present excitation wavelength dependent fluorescence measurements suggest that the linker

chain length in the dicationic moiety plays important role in determining the micro-heterogeneous nature of the dicationic ionic liquid.

3.3. Solvation dynamics study

The emission decay profile of C153 at magic angle (54.7^0) are collected at several wavelengths (5–10 nm intervals) across the emission spectra by exciting the sample at 375 nm, 405 nm and 445 nm at different temperatures. The decay profiles are found to be strongly dependent on the monitoring wavelengths (Fig. S3, ESI†). The observation of a faster decay at shorter monitoring wavelengths and a clear rise with usual decay at longer monitoring wavelength indicate the typical signature of solvation process.[69] The time-resolved emission spectra (TRES) of the system, constructed from the fitted decay profiles, show progressive red shift of the fluorescence maximum with time. Construction of TRES is repeated twice to verify the reproducibility of the result. Representative TRES of C153 in $[C_6(MIm)_2][NTf_2]_2$ is shown in Fig. 4(a). The earlier TRES plot is provided in the supporting information (Fig. S4). In all the cases time dependent shifts of the emission maximum to lower energy have been observed which indicates solvent stabilization of excited state of the dipolar probe molecule with time. From Fig. 4(b), one can see that the FWHM (full width at half maxima) decreases by a factor of ~1.5 from 0 ps to 3500 ps. As the narrowing seems to be the result of loss of intensity only at one end (the high energy side) of the spectrum, it is suggestive of an additional relaxation pathway. In this context we would like to mention that the present observation is not surprising and Maroncelli and his coworkers [34] have indeed observed similar behavior while studying dynamics of solvation of C153 in some monocationic ILs. During investigation a ~45% narrowing of the spectra has been observed by

them. They have attributed the spectral narrowing is mainly due to vibrational cooling.[34] However, since the time-scale is also an important factor, the change in local solvation environment may contribute to the narrowing down of the FWHM in the present case.[75] Here, we want to mention that the synthesized dicationic IL is vigorously purified and the purity has been checked by ^{1}H- NMR spectroscopy (Fig S1, ESI†) and mass spectrometry. Viscosity value of dicationic IL is also found to be comparable with the literature data.[55] Hence, any role of impurity in the dicationic IL towards narrowing of TRES can be completely ruled out. However, at this point, we are not in a position to conclusively comment about the exact reason for the large narrowing down of the FWHM of TRES. More experiments are needed to get a concrete reason behind such observation.

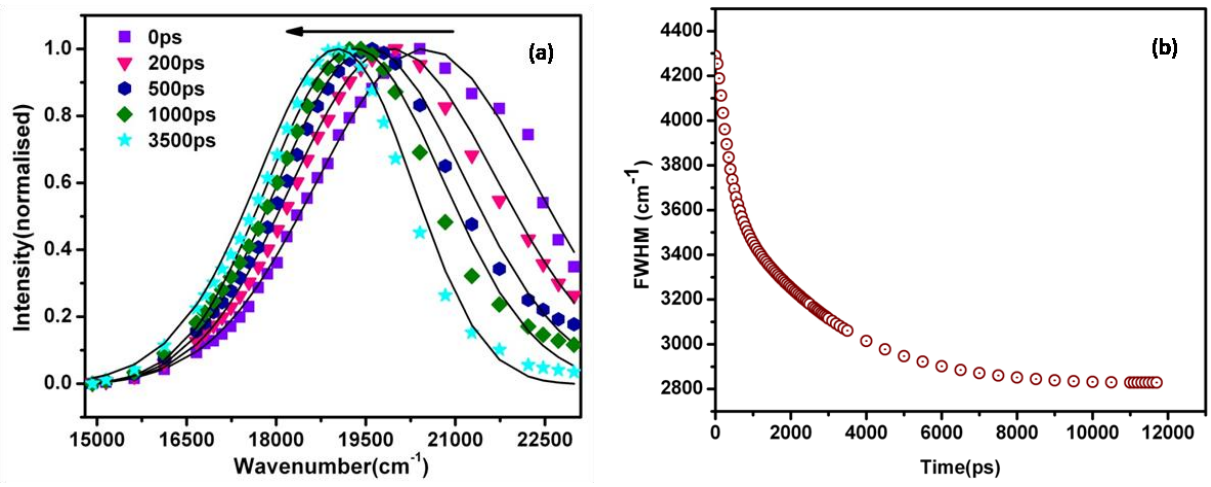

Fig. 4. TRES of C153 in [C_6MIm][NTf_2] at different time at 293K (λ_{exc}=405nm) (a). All spectra are normalized at their corresponding peak maxima. Variation of FWHM (full width at half maxima) of TRES with time (b).

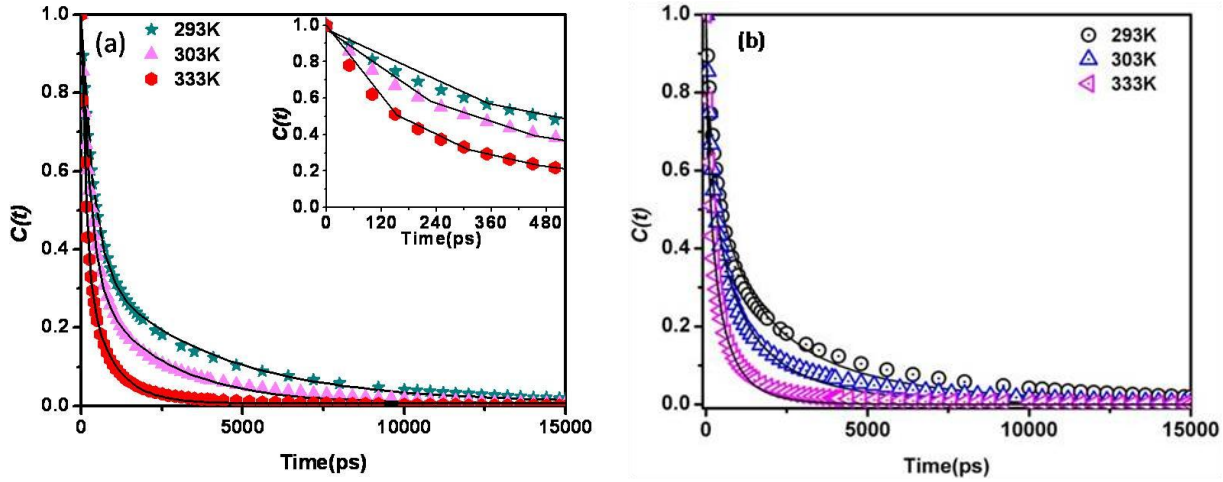

Fig. 5. Decay of the spectral shift correlation function, *C(t)* of C153 in $[C_6(MIm)_2][NTf_2]_2$ with 405 nm as excitation source. (a) Bi-exponential fit to the data points with solid black lines. Inset shows decay within first 500ps. (b) Stretched exponential fit to the data points with solid black lines.

The time constants of the observable dynamics are determined from the plots of the spectral shift correlation function, *C(t)*, versus time. Representative plots of *C(t)* versus time for C153 in $[C_6(MIm)_2][NTf_2]_2$ at $\lambda_{exc.}$ = 405 nm are shown in Fig. 5. Both biexponential (Fig. 5(a)) and stretched exponential (Fig. 5(b)) fitting are done to the *C(t)* versus time plots. Average solvation times are found to be very similar on both occasions. However, biexponential description provides better fit to the data. The detailed solvation parameters at different temperatures are collected in Table 1. It is noticeable from Table 1 that with the increase in temperature the average solvation time ($<\tau_s>$) decreases. The observation can be attributed to the gradual lowering of bulk viscosity of the medium with rise in temperature.[8] Moreover, when weighted components of average solvation time are plotted against the bulk viscosity values of the IL (Fig. 6), long weighted slow components are found to correlate linearly with the bulk viscosity of the medium, whereas the fast components show much less changes with increase in the viscosity of the medium. The observation indicates that the average solvation rate is dominated by viscosity

change. The similar behavior has also been observed for monocationic imidazolium-based ionic liquids.[8]

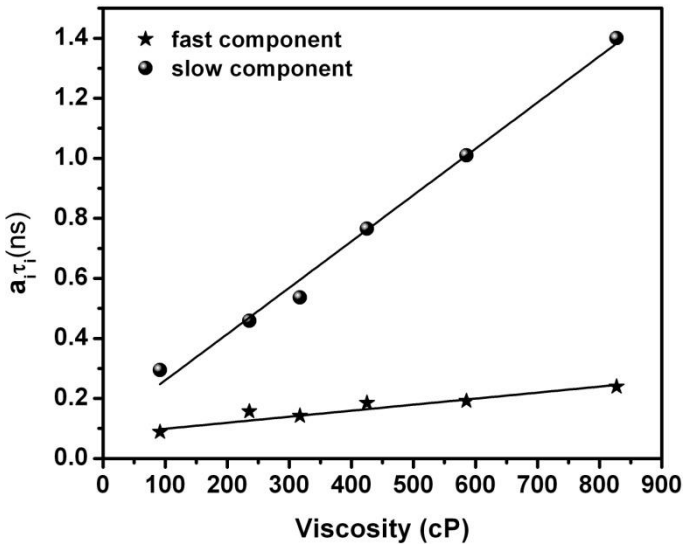

Fig. 6. Plot of weighted components of solvation time vs. viscosity for $[C_6(MIm)_2][NTf_2]_2$.

Table 1. Solvation relaxation parameters of C153 in $[C_6(MIm)_2]$ $[NTf_2]_2$ at $\lambda_{exc.}$ = 405nm at different temperatures.

Vis.(cP)/ Temp.(K)	Biexponential Fit[a]								Stretched exponential Fit[b]		
	a_1	τ_1(ns)	a_2	τ_2(ns)	$<\tau_s>$(ns)	$\Delta\nu_{obs}$ (10^3cm^{-1})	$\Delta\nu_{est}$ (10^3cm^{-1})	f_{obs}	β	τ_{sol}(ns)	$\langle\tau_{st}\rangle$(ns)
827/293	0.64	0.37	0.36	3.89	1.64	1.64	1.43	1.15	0.57	0.94	1.53
585/298	0.63	0.30	0.37	2.73	1.20	1.65	1.42	1.16	0.57	0.74	1.19
425/303	0.67	0.28	0.33	2.32	0.95	1.61	1.40	1.15	0.58	0.59	0.92
317/308	0.69	0.21	0.31	1.73	0.68	1.71	1.43	1.19	0.59	0.42	0.64
235/313	0.72	0.22	0.28	1.64	0.60	1.53	1.43	1.07	0.64	0.40	0.57
92/333	0.64	0.12	0.36	0.82	0.38	0.95	1.40	0.67	0.65	0.28	0.38

[a] biexponential fit according to equation 4 and [b] stretched exponential fit according to equation 6. $\Delta\nu_{obs}$ is the observed dynamic shift calculated time resolved solvation data. $\Delta\nu_{est}$ is the difference between $\nu(\infty)$ from the fits and the time-zero frequency estimated according to the methods of ref 76 and $f_{obs} = \Delta\nu_{obs}/\Delta\nu_{est}$. Experimental error ± 5%.

To get more insight into the viscosity dependence of average solvation time, we have further analyzed the results by fitting average solvation time with the relationship $<\tau_s> \propto (\eta/T)^p$ (p is the exponent and T is the temperature)[46] where (η/T) is the temperature-reduced bulk viscosity. The exponent, p, when estimated from solvent relaxation data (Eq. 9) is found to be (p = 0.77).

C153 in $[C_6(MIm)_2][NTf_2]_2$, $\log(<\tau_s>) = (-0.142) + 0.77 \log(\eta/T)$ (9)

The observation indicates that there is appreciable decoupling of average solvation time from medium viscosity, a phenomenon believed to be caused due to the medium dynamic heterogeneity.[46] We have also calculated the missing component of the dynamics by Fee-Maroncelli method.[76] The observed dynamic shift ($\Delta\nu$) is found to be close to the expected value ($\Delta\nu_{est}$) (Table 1). It may be mentioned in that context that the observed shift in the dicationic IL (1650cm^{-1}) is higher than the shift reported for isopolar DCM (1220cm^{-1}) [72]. This data probably indicates the solvation dynamics in ILs is quite different from that in conventional solvents and correlating solvation dynamics with only the dielectric constant value may not be sufficient. In this context we would also like to mention that Maroncelli and co-workers[34] have detected frequency shift of C153 in monocationic IL to be 1850 cm-1 (at 293 K, 400 nm excitation wavelength), which is higher than the detected frequency shift (1320 cm-1 at 293K, 405 nm excitation wavelength) of the same in the present study. The study by Maroncelli and co-workers involves a combination of fluoresecence upconversion (FLUPS) and TCSPC technique which detects the complete dynamics which spans from sub-picosecond to nanosecond. The better time resolution provided by the FLUPS enabled detection of the initial fast component which amounts to ~20-30% of the total dynamics. In our study we have used the TCSPC technique only and thus missed completely this fast part for the mono-cationic IL.

From the f_{obs} value in Table 1, one can infer that essentially there is no ultrafast solvation component for dicationic system. However, at low viscous condition (last row Table 1) ~32% missing solvation component is observed. The present observation is also interesting in a sense that the absence of missing component in solvation dynamics has only been observed in case of highly viscous phosphonium ionic liquid.[33] The factor responsible for such observation might be related to the slow orientation of the bulky dication around the excited probe molecules. In this context Nishikawa et al.[77] while studying the dynamics of cation and anion rotation in 1-butyl-3-methylimidazolium hexafluorophosphate ($[C_4mim]PF_6$) using multinuclear NMR spectroscopy have shown that the butyl chain reorientation motions are slower than the imidazolium ring reorientation. They have also observed that a decoupling of rotational dynamics of the PF_6^- anions and $[C_4mim]^+$ cations. In a separate work on quasielastic neutron scattering (QENS) on 1-butyl-3-methylimidazolium chloride ($[C_4mim]Cl$) by Hamaguchi et al.[78] have demonstrated that the motion of $[C_4mim]^+$ ion is simple diffusion and the flexibility of the cation stabilizes the IL entropically. Based on the above results it is reasonable to infer that the restricted motion of the two imidazolium ring in the dication due to hexyl linker chain might be responsible for slowing down the reorientation of the dication around the probe molecule. The data for monocationic system shows that at 293 K ~20% of the dynamics is missed (Table S1, ESI†). We would also like to note that imidazolium monocationic ionic liquids generally exhibit significant amount of fast solvation component.[13] The observation points that nature of cation plays a significant role in controlling the ultrafast component that is generally being observed in these media. The absence of ultrafast component in case of dicationic ionic liquid possibly indicates that the origin of ultrafast component is related to the dipolar rotation of the imidazolium cation the findings that has been already discussed in a few recent studies.[39-42] However, we would also like to stress

that further investigation possibly exploiting molecular dynamics simulation might be required to rationalize the observed behavior.

We would like to point out that the observation of more frequency shift than the estimated one (Table 1) in the present case (having time resolution of the TCSPC setup ~75 ps) is not surprising. Fee-Maroncelli method is an approximate one where time-zero spectrum is estimated by deducting the steady state Stokes shift of the same probe in a non-polar reference solvent from the absorption spectrum of that probe in the given polar solvent of interest. This is done to approximately account for the extra-stabilization induced by the interaction between the excitation-induced enhanced dipole moment of the solute and the surrounding solvent molecules which are still 'frozen' in the configuration when the solute was in its ground state. Subtraction of the Stokes shift derived from a non-polar reference solvent therefore takes care of the density effect (electronic part of the solvent polarization) with the assumption that the underlying vibronic structure of the probe remains unaltered regardless of the state of the probe (ground or excited) and the character of the solvent used (polar, non-polar, ionic, confined etc.). For normal solvents at room temperature, the density of polar and non-polar solvents do not differ greatly, and as a result, the error due to density difference becomes negligible while estimating the 'true' shift using the Fee-Maroncelli method for common dipolar solvents at normal or close to normal condition. However, the error can become large when the density of the non-polar reference becomes different from the polar medium under investigation; this is exactly the case for our IL systems. The effect of density has also been observed not only in solvation in bulk liquids but also in confined system[79]. The density of $[C_6(MIm)_2][NTf_2]_2$ as reported by Anderson and co-workers [51] is 1.52 gm/cm^3 is quite different from the density of the nonpolar reference cyclohexane (0.79gm/cm^3). It may be noted here that these data are reproducible. Examples of

detected shifts being a few percent larger than the estimated 'true' values can be found even in works performed with ~25 ps resolution in ILs.[33] Similar observation has also been obtained by Biswas & coworkers such in (amide + electrolyte) deep eutectics.[39] Therefore, detected shift being slightly larger than the estimated true shift merely indicate that the full detection of the dynamic Stokes shift.

We have also estimated the specific conductivities of both ILs. In the present case, the specific conductivity values for $[C_6(MIm)_2][NTf_2]_2$ and $[C_6MIm][NTf_2]$ at isoviscous (92 cp) condition are estimated to be 0.140 Sm^{-1} and 0.072 Sm^{-1} respectively. Considering the Maroncelli's latest work (average solvation time of a dipolar solute is inversely proportional to the electrical conductivity of the medium) [36] it may be inferred that the higher conductivity for dicationic IL is basically responsible for observed faster solvation time in that medium than that of monocationic IL of same viscosity. However, the correlation between solvation time and inverse conductivity found for neat ILs breaks down for binary (IL+ polar solvent) mixtures.[31] Theoretical studies on binary (IL + polar solvent) mixtures by Biswas and coworkers,[39] have indeed predicted deviation from linear correlation between average solvation times and inverse conductivity, and validity of this linear relationship for neat ILs. Interestingly, the theoretical calculations presented by Biswas and coworkers did not use conductivity at any point of their calculations (instead they used viscosity). This is an interesting aspect and needs further investigation.

We have also calculated activation energy associated with the solvation process ($E_a(<\tau_s>)$) for both mono and dicationic IL, by fitting the solvation times to the natural logarithm of the Arrehnius type expression $\langle\tau_s\rangle = A \exp[Ea/RT]$. The activation energies of solvation for mono and dicationic IL are found to be 30.7 and 40.5 $kJmol^{-1}$ respectively. The data in monocationic IL matches well with theoretically calculated value of $E_a(\langle\tau_{se}\rangle)$ (33.9 $kJmol^{-1}$) by Kashyap and

Biswas[43] where $\langle\tau_{se}\rangle$ is the average solvation time calculated from solvation energy time autocorrelation function. Similarly the data for dicationic IL matches with that of [hmim][BF_4] (40.6 kJmol^{-1}) which has the highest activation energy among the series of RTIL studied by the authors.[43]

We would like to mention here that the solvation data shown in Table 1 and Fig. 6, and rotation data in Table 2 and Fig. 8 have been obtained by using a single excitation wavelength (λ_{exc}=405nm) for C153 dissolved in the dicationic IL, $[C_6(MIm)_2][NTf_2]_2$. While Fig. 6 and Table 1 display solvation data obtained at six different temperatures, the rotation data in Fig. 8 correspond to nine different temperatures. These data provide nice correlations with temperature-scaled viscosity (η/T) (as reflected in the corresponding plots). Therefore, the current set of data is sufficient to bring out the qualitative behavior of the solvent coupling to the solute-centered dynamics (that is, solute solvation and rotation) in this dicationic IL. Data at few other temperatures would better the statistics only without having any impact of the qualitative understanding of solute-solvent coupling in this medium brought out here by the current data set.

It may also be mentioned that Fig. 3 present results of our study on steady state excitation wavelength dependence of fluorescence emission of a dissolved solutes in mono and dicationic ILs. These results highlight very similar and weak λ_{exc} dependence of fluorescence emission in these ILs. More importantly, the extent of λ_{exc} dependence does not change even if probes with very different lifetimes are used (supplementary information). The corresponding results from λ_{exc} dependent fluorescence dynamics investigation are provided in the supplementary information. Our λ_{exc} dependent dynamic study is limited but is sufficient to indicate the micro-heterogeneous nature of this IL.

3.4. Time-resolved fluorescence anisotropy study

We have also investigated the rotational diffusion behavior of C153 in the dicationic IL. Representative time resolved fluorescence anisotropy decay profile of C153 in the RTIL is shown in Fig. 7. Table 2 lists the rotational relaxation parameters of C153 in dicationic IL at different temperatures. The anisotropy decay profiles are fitted to a bi-exponential function. As can be seen from Table 2, the average rotational relaxation time ($<\tau_r>$) decreases with increase in temperature. The lowering of average solvation time upon increasing the temperature is caused due to the lowering of the medium viscosity upon increase in temperature.

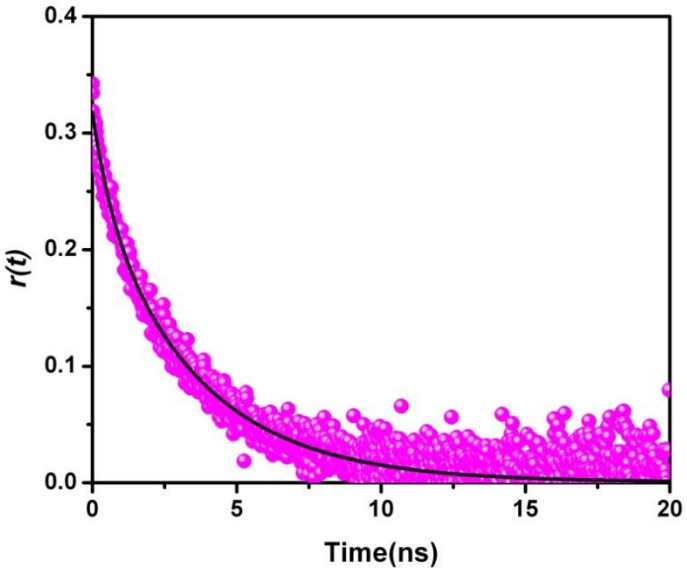

Fig. 7. Time resolved fluorescence Anisotropy decay (TRFAD) for C153 in $[C_6(Mim)_2]$ $[NTf_2]_2$ at 333K. Solid line in the figure represents the biexponential fit to the data points.

Table 2. Rotational Relaxation Parameter of C153 in $[C_6(MIm)_2]$ $[NTf_2]_2$ at $\lambda_{exc.}$ = 405 nm

Temp.(K)	Viscosity	[a]r_0	a_1	τ_1(ns)	a_2	τ_2(ns)	$<\tau_r>$(ns)
293	827	0.32	0.17	1.32	0.83	17.78	14.98
298	585	0.31	0.16	1.36	0.84	14.48	12.32
303	425	0.32	0.17	1.01	0.83	12.46	10.49
308	317	0.32	0.17	1.03	0.83	9.44	7.99
313	235	0.32	0.19	1.10	0.81	7.95	6.64
318	183	0.33	0.2	1.04	0.8	6.59	5.48
323	144	0.33	0.24	1.20	0.76	5.69	4.61
328	115	0.32	0.24	1.11	0.76	4.64	3.79
333	92	0.34	0.21	0.65	0.79	3.51	2.93

[a]r_0 is the initial anisotropy. Experimental error 5-10%.

The viscosity dependence of average rotational relaxation data have been further analyzed by plotting $\log<\tau_r>$ vs. $\log(\eta/T)$ along with the stick and slip boundary condition (Fig. 8).

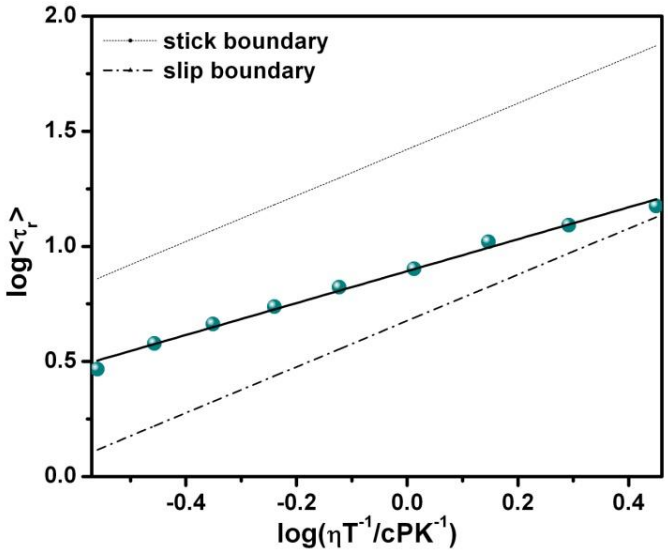

Fig. 8. The log-log plots of $<\tau_r>$ vs. η/T. The solid line is the linear fit to the data points.

From Fig. 8, it is evident that the rotational diffusion behavior of C153 in the dicationic IL lie well within the boundary conditions set by SED (Stokes-Einstein-Debye) hydrodynamic theory.[70] However, when we further analyze the results by applying the relation: $\langle \tau_r \rangle \propto (\eta/T)^p$ (r being rotation, p is the exponent and T is the temperature) The exponent, p, is estimated to be 0.69. It may be noted here that the decoupling of solvation dynamics and solute rotation from the medium viscosity is manifested through fractional viscosity (η) dependence of the measured average solvation $\langle \tau_s \rangle$ and rotation $\langle \tau_r \rangle$ times.[46,70,80-81] Moreover, it has been also found that medium heterogeneity is primarily responsible for the observed viscosity-diffusion (d-η) decoupling behavior.[46,80-81] From Table 2 one can see that the rotational time constants at lower temperatures (293K and 298K) are about 3-5 times of the excited state lifetime of C153 (4-5ns). Similar high rotational time constants have also been observed by Castner and co-workers [27] in pyrrolidinium ILs, *N*-methyl-*N*-butylpyrrolidinium bis(trifluoromethylsulfonyl)imide ($Pyrr_{14}^+/NTf_2^-$), and *N*-methyl-*N*-ethoxyethylpyrrolidinium bis(trifluoromethylsulfonyl)imide ($Pyrr1_{(2O2)}^+/NTf_2^-$). The authors have reasoned that the nanostructural domains present in the ILs might be the responsible for such behavior. Such nanostructural domains can restricts the rotation of the probe. Similar argument can be stated in the present case where at lower temperature rotation of the probe is hindered by the nanostructural organizations which changes at higher temperature. Very recently, we have seen that rotational relaxation dynamics of C153 is found to be intermediate between other two solutes, nonpolar perylene and the charged sodium 8-methoxypyrene-1,3,6-sulfonate (MPTS), in both $[C_6(MIm)_2][NTf_2]_2$ and $[C_6Mim][NTf_2]$.[82] Such a behavior indicates that C153 is distributed in both polar and nonpolar region of the media. In general, other than the viscosity effect, the rotational relaxation behavior of C153 is observed to be similar with imidazolium monocationic-based IL (Table S4, ESI†).

5 Conclusion

In the present report solvation and rotational relaxation dynamics of Coumarin 153 have been investigated in a dicationic ionic liquid, $[C_6(MIm)_2][NTf_2]_2$, for the first time. Several interesting features with regard to understanding the fundamentals of solvation dynamics have come out from the present study. (1) Steady state spectral measurements reveal that the polarity of the ionic liquids is very similar and close to that of dichloromethane. (2) Excitation wavelength dependent steady–state fluorescence measurements reveal micro-heterogeneous behavior of the dicationic IL. Excitation wavelength dependent fluorescence measurements reveal that the extent of microheterogeneity is quite similar to a structurally similar monocationic ionic liquid, $[C_6MIm][NTf_2]$. Presence of similar nonpolar alkyl chain in both ILs is perhaps responsible for very similar microhetrogeneious nature of the two media. (3) An interesting finding is that no ultra-fast component of solvation has been observed in case of dicationic system. Such behavior has not been observed for monocationic imidazolium-based ionic liquid. We believe that the absence of ultrafast component in dicationic ionic liquid indicates a close relationship exists between cationic moiety and ultrafast solvation component. However, further investigations such as molecular dynamics simulation may be required to understand such behavior.

Acknowledgments

This work was supported by the Department of Science and Technology (DST), Government of India. S. K. D. thanks the Council of Scientific and Industrial Research (CSIR), New Delhi for awarding a fellowship. P. K. S thanks National Institute of Science Education and Research (NISER), Bhubaneswar for a fellowship.

Keywords: Ionic liquids, heterogeneity, solvation dynamics, ultra-fast components, rotational diffusion

† Electronic supplementary information (ESI) available: Proton NMR spectrum for $[C_6(MIm)_2][NTf_2]_2$ in DMSO-d_6, excitation wavelength dependent fluorescence response of ANF and C153 in $[C_6(MIm)_2][NTf_2]_2$ at 298K, time-resolved fluorescence decay profiles of C153 in $[C_6(MIm)_2][NTf_2]_2$ at 293K (λ_{exc}=405nm), earlier TRES of C153 in $[C_6MIm][NTf_2]$ at different time at 293K (λ_{exc}=405nm), solvation relaxation parameters of C153 in $[C_6MIm][NTf_2]$ at $\lambda_{exc.}$ = 405nm at different temperatures, Solvation relaxation parameters of C153 at 291K in $[C_6MIm][NTf_{2.}]$, solvation relaxation parameters of C153 at 333K in $[C_6(MIm)_2][NTf_2]_{2,}$ rotational Relaxation Parameter in $[C_6(MIm)_2][NTf_2]_2$ and $[C_6Mim][NTf_2]$ at different excitation wavelengths.

References

1 P. Wasserscheid and T. Welton, *Ionic Liquids in Synthesis*, 2nd ed., Eds Wiley, VCH, Weinheim, 2008.

2 H. Ohno, *Electrochemical Aspects of Ionic Liquids* (Ed.; Wiley-Interscience: Hoboken, NJ, 2005).

3 K. R. Seddon, *J. Chem. Technol. Biotechnol.* 1997, **68**, 351-356.

4 T. Welton, *Chem. Rev.* 1999, **99**, 2071-2084.

5 M. Freemantle, *Chem. Eng. News.* 2007, **85**, 23-26.

6 B. Bagchi, B. Jana, *Chem. Soc. Rev.* 2010, **39**, 1936-1954.

7 A. Samanta, *J. Phys. Chem. B* 2006, **110**, 13704-13716.

8 A. Samanta, *J. Phys. Chem. Lett.* 2010, **1**, 1557-1562.

9 B. Lang, G. Angulo and E. Vauthey, *J. Phys. Chem. A* 2006, **110**, 7028-7034.

10 S. Arzhantsev, H. Jin, G. A. Baker and M. Maroncelli, *J. Phys. Chem. B* 2007, **111**, 4978-4989.

11 Y. Kimura, M. Fukuda, K. Suda and M. Terazima, *J. Phys. Chem. B* 2010, **114**, 11847-11858.

12 M. Muramatsu, Y. Nagasawa and H. Miyasaka, *J. Phys. Chem. A* 2011, **115**, 3886-3894.

13 H. Jin, X. Li and M. Maroncelli, *J. Phys. Chem. B* 2007,**111**, 13473-13478.

14 E. W. Castner, Jr., C. J. Margulis, M. Maroncelli and Wishart James, F. *Annu. Rev. Phys. Chem.* 2011, **62**, 85-105.

15 K. Sahu, S. J. Kern and M. A. Berg, *J. Phys. Chem. A* 2011, **115,** 7984-7993.

16 P. K. Mandal, M. Sarkar and A. Samanta, *J. Phys. Chem. A* 2004, **108**, 9048-9053.

17 A. Paul and A. Samanta, *J. Phys. Chem. B* 2007, **111**, 4724-4731.

18 D.C. Khara and A. Samanta, *J. Phys. Chem. B* 2012, **116**, 13430-13438.

19 Y. Shim and H. J. Kim, *J. Phys. Chem. B* 2008, **112**, 11028-11038.

20 M. N. Kobrak, *J. Chem. Phys.* 2007, **127**, 184507/1-184507/8.

21 M. N. Kobrak, *J. Chem. Phys.* 2006, **125**, 064502.

22 N. Ito, S. Arzhantsev and M. Maroncelli, *Chem. Phys. Lett.* 2004, **396**, 83-91.

23 D. Roy and M. Maroncelli, *J. Phys. Chem. B* 2012, **116**, 5951-5970.

24 S. Daschakraborty and R. Biswas, *J. Chem. Phys.* 2012, **137**, 114501.

25 X. Song, *J. Chem. Phys.* 2009, **131**, 044503/1-044503/8.

26 M. Maroncelli, X.-X. Zhang, M. Liang, D. Roy and N. P. Ernsting, *Faraday Discuss. Chem.Soc.* 2012, **154**, 409-424.

27 A. M. Funston, T. A. Fadeeva, J. F. Wishart and E. W. Castner, Jr. *J. Phys. Chem. B* 2007, **111**, 4963-4977.

28 A. Adhikari, K. Sahu, S. Dey, S. Ghosh, U. Mandal and K. Bhattacharyya, *J. Phys. Chem. B* 2007, **111**, 12809-12816.

29 S. Dey, A. Adhikari, D. K. Das, D. K. Sasmal, and K. Bhattacharyya, *J. Phys. Chem. B* 2009, **113**, 959-965.

30 D. K. Sasmal, S.S. Mojumdar, A. Adhikari, and K. Bhattacharyya, *J. Phys. Chem. B* 2010, **114**, 4565-4571.

31 X.-X. Zhang, M. Liang, J. Hunger, R. Buchner and M. Maroncelli, *J. Phys. Chem. B.* 2013, **117**, 15356-15368.

32 S. Sarkar, R. Pramanik, C. Ghatak, P. Setua and N. Sarkar, *J. Phys. Chem. B.* 2010, **114**, 2779-2789.

33 N. Ito, S. Arzhantsev, M. Heitz and M. Maroncelli, *J. Phys. Chem. B* 2004, **108**, 5771-5777.

34 X.-X. Zhang, M. Liang, N. P. Ernsting and M. Maroncelli, *J. Phys. Chem. B.* 2013, **117**, 4291-4304.

35 X.-X. Zhang, C. Schröder and N. P. Ernsting, *J. Chem. Phys.* 2013, **138**, 111102/1-11103/3.

36 X.-X. Zhang, M. Liang, N.P. Ernsting and M. Maroncelli, *J. Phys. Chem. Lett.* 2013, **4**, 1205-1210.

37 M. Halder, L. S. Headley, P. Mukherjee, X. Song and J. W. Petrich, *J. Phys. Chem. A* 2006, **110**, 8623-8626.

38 P. J. Carlson, S. Bose, D. W. Armstrong, T. Hawkins, M. S. Gordon and J. W. Petrich, *J. Phys. Chem. B* 2012, **116**, 503-512.

39 S. Daschakraborty and R. Biswas, *J. Phys. Chem. B* 2014, **118**, 1327-1339.

40 T. Pal and R. Biswas, *Theor. Chem. Acc.* 2013, **132**, 1348/1.

41 S. Daschakraborty and R. Biswas, *Chem. Phys. Lett.*, 2011, **510**, 202-207.

42 H. K. Kashyap and R. Biswas, *J. Phys.Chem. B*, 2010, **114**, 254-268.

43 H. K. Kashyap and R. Biswas, *J. Phys.Chem. B*, 2010, **114**, 16811-16823.

44 S. K. Das and M. Sarkar, *Chem.Phys. lett* 2011, **515**, 23-28.

45 S. K. Das and M. Sarkar, *Chem Phys Chem* 2012, **13,** 2761-2768.

46 S. K. Das, P.K. Sahu and M. Sarkar, *J. Phys. Chem. B* 2013, **117**, 636-647.

47 V. Gangamallaiah and G. B. Dutt, *J. Phys. Chem.B* 2013, **117**, 12261-12267.

48 D. C. Khara, J. P. Kumar, N. Mondal and A. Samanta, *J. Phys. Chem.B* 2013, **117**, 5156-5164.

49 B. Li, M. Qiu, S. Long, X. Wang, Q. Guo and A. Xia, *Phys. Chem. Chem. Phys*. 2013, **15**, 16074-16081.

50 B. Li, Y. Wang, X. Wang, S. Vdovic, Q. Guo, A. Xia *J Phys Chem B* 2012, *116*,13272-13281.

51 J. L. Anderson, R. Ding, A. Ellern and D. W. Armstrong, *J. Am. Chem. Soc.* 2005, **127**, 593-604.

52 T. Payagala, J. Huang, Z. S. Breitbach, P. S. Sharma and D. W. Armstrong, *Chem. Mater.* 2007, **19**, 5848.

53 Y.-S. Ding, M. Zha, J. Zhang and S.-S. Wang, *Colloids Surf. A* 2007, **298**, 201-205.

54 H. Sun, D. Zhang, C. Liu and C. Zhang, *THEOCHEM* 2009, **900**, 37-43.

55 H. Shirota, T. Mandai, H. Fukazawa and T. Kato, *J. Chem. Eng. Data* 2011, **56**, 2453-2459.

56 S. I. Lall, D. Mancheno, S. B. Castro, J. I. Cohen and R. Engel, Polycations. Part X. LIPs, *Chem. Commun*. 2000, 2413-2414.

57 R. Engel, J. I. Cohen and S. I. Lall, *Phosphorus, Sulfur Silicon Relat. Elem*. 2000, **177**, 1441-1445.

58 R. Engel, and J. I. Cohen, *Curr. Org. Chem* 2002**, 6**, 1453-1467.

59 J. F. Wishart, S. I. Lall-Ramnarine, R. Raju, A. Scumpia, S. Bellevue, R. Ragbir and R. Engel, *Radiat. Phys. Chem.* 2005, **72**, 99-104.

60 M. Yoshizawa, K. Ito-Akita and H. Ohno, *Electrochim. Acta* 2000, **45**, 1617-1621.

61 K. Ito, N. Nishina and H. Ohno, *Electrochim. Acta* 2000, **45**, 1295-1298.

62 S. Yeganegi, A. Soltanabadi and D. Farmanzadeh, *J. Phys. Chem. B* 2012, **116**, 11517-11526.

63 T. Ishida and H. Shirota, *J. Phys. Chem. B* 2013, **117**, 1136-1150.

64 B. L. Bhargava and M. L. Klein, *J. Chem. Theory Comput.* 2010, **6**, 873,

65 E. Bodo, M. Chiricotto and R. Caminiti, *J. Phys. Chem. B* 2011, **115**, 14341,

66 S. Li, G. Feng, J. L. Bañuelos, G. Rother, P. F. Fulvio, S. Dai and P.T. Cummings, *J. Phys. Chem. C* 2013, DOI: 10.1021/jp406381g

67 H. Shirota and T. Ishida, *J. Phys. Chem. B* 2011, **115**, 10860-10870.

68 M. N. Kobrak and H. Li, *Phys. Chem. Chem. Phys.* 2010, **12**, 1922-1932.

69 M. Maroncelli and G. R. Fleming, *J. Chem. Phys.* 1987, **86**, 6221.

70 C. M. Hu and R. Zwanzig, *J. Chem. Phys.* 1974, **60**, 4354.

71 S. K. Das and M. Sarkar, *J. Phys. Chem. B* 2012,**116**, 194-202.

72 M. L. Horng, J. A. Gardecki, A. Papazyan and M. Maroncelli, *J. Phys. Chem.* 1995, **99**, 17311-17337.

73 B. Valeur and G. Weber, *Chem. Phys. Lett.* 1977, **45**, 140-144.

74 G. Weber and M. Shinitzky, Proc. Natl. Acad. Sci. U.S.A. 1970, **65**, 823-830.

75 A. Halder, S. Sen, A. D. Burman, A. Patra and K. Bhattacharyya, *J. Phys. Chem. B*, 2004, **108**, 2309-2312.

76 R.S. Fee and M. Maroncelli, *Chem. Phys.* 1994, **183**, 235-247.

77 T. Endo, S. Widgeon, P. Yu, S. Sen and K. Nishikawa, *PHYSICAL REVIEW B* 2012, **85**, 054307.

78 Y. Inamura, O. Yamamuro, S. Hayashi and H. Hamaguchi, *Physica B* 2006, **385**, 732–734.

79 B. Guchhait, R. Biswas and P. K. Ghorai, *J. Phys. Chem. B* 2013, **117**, 3345−3361

80 B. Guchhait, S. Das, S. Daschakraborty and R. Biswas, *J. Chem. Phys.* 2014, **140**, 104514.

81 T. Pal and R. Biswas, *Chem.Phys. lett* 2011, **517**, 180-185.

82 P.K. Sahu, S. K. Das and M. Sarkar, *J. Phys. Chem. B* 2014, **118**, 1907-1915.

TOC Image

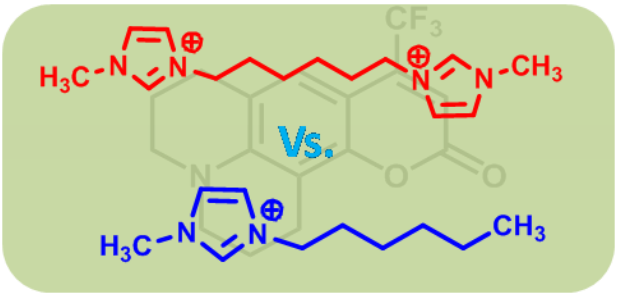

Solvation dynamics of coumarin 153 is compared in di and in mono-cationic-based ionic liquids for the first time.